arXiv:0908.1228v1 [cond-mat.mtrl-sci] 9 Aug 2009

Randomness-Induced Redistribution of Vibrational Frequencies in Amorphous Solids

Valery Ilyin[1], Itamar Procaccia[1], Ido Regev[1] and Yair Shokef[2]
[1]*Department of Chemical Physics,* [2] *Department of Physics of Complex Systems,*
The Weizmann Institute of Science, Rehovot 76100, Israel
(Dated: August 10, 2009)

Much of the discussion in the literature of the low frequency part of the density of states of amorphous solids was dominated for years by comparing measured or simulated density of states to the classical Debye model. Since this model is hardly appropriate for the materials at hand, this created some amount of confusion regarding the existence and universality of the so- called "Boson Peak" which results from such comparisons. We propose that one should pay attention to the different roles played by different aspects of disorder, the first being disorder in the interaction strengths, the second positional disorder, and the third coordination disorder. These have different effects on the low-frequency part of the density of states. We examine the density of states of a number of tractable models in one and two dimensions, and reach a clearer picture of the softening and redistribution of frequencies in such materials. We discuss the effects of disorder on the elastic moduli and the relation of the latter to frequency softening, reaching the final conclusion that the Boson peak is not universal at all.

I. INTRODUCTION

The study of the density of states of solid materials started with attempts to understand the temperature dependence of the specific heat at low temperatures, say $C_V \equiv (\partial U/\partial T)_V$ where U is the energy and T the temperature of the system. This called for a microscopic theory for solids, and the first one was developed by Einstein, assuming that in d dimensions each atom is represented as a d-dimensional harmonic oscillator [1] (in the original paper the case $d = 3$ was considered). In this article Planck's quantization assumption, which was originally applied to radiation, was extended to solid vibrations [2]. In the case of dN linear oscillators each with its own frequency ω_i, Einstein's result can be expressed as

$$C_V = dNk_B \int_0^\infty \left(\frac{\hbar\omega}{2k_BT}\right)^2 csch^2\left(\frac{\hbar\omega}{2k_BT}\right) g(\omega)\mathrm{d}\omega \ . \quad (1)$$

Here k_B and $\hbar$ are Boltzmann's and Planck's constants respectively, and the density of states $g(\omega)$ is defined by

$$g(\omega) = \frac{1}{dN}\sum_i^{dN} \delta(\omega - \omega_i) \quad (2)$$

where $\delta(x)$ is the delta function.

Both the theoretical calculation and experimental measurement of $g(\omega)$ attracted enormous attention over the last century. We are interested in amorphous system like glasses, gels, foams etc., in which randomness appears to influence the low-frequency part of the density of states $g(\omega)$. In particular the relation between the low-frequency behavior and the low-temperature thermodynamics of such systems is of great interest. Studies of the low-frequency part of the density of states are dominated by dividing $g(\omega)$ by the prediction of the Debye model, focusing on the deviation between the two, and in particular on the so-called "Boson peak" which emerges in many cases. There exist numerous claims about the Boson peak, its universality [3] and its relation to softening or hardening of the materials under changes of material parameters [4]. In this paper we first explain the classical approaches to the issue, including the Debye model and beyond, and then we examine the issue of universality of the Boson peak in one and two dimensions using tractable models that can be computed to desired accuracy. We conclude that there is nothing universal about the Boson peak, and that different types of disorder result in very different redistributions of the low-frequency modes over the spectral domain. There is in general no correlation between the size or the position of the Boson peak and the increase or decrease of elastic moduli.

The structure of this paper is as follows: In Section II we review Debye's theory and the historical origins of the Boson peak. In Section III we remind the reader what is entailed in computing the density of states by solving the appropriate eigenvalue equation. We then remind the reader that even for a perfect cubic crystal the Debye model is not exact, with corrections at frequencies which become lower as the material gets softer. To understand the effect of disorder in the inter-particle forces we review some known results and present some new results for one-dimensional chains in Section IV. In Section V we discuss tractable models of disorder in two dimensions, aiming to better model the typical disorder exhibited by glass-forming systems. We first examine the effects of disorder in the spring-constants or, equivalently, in the positions of the particles. Second, we consider disorder in the coordination numbers (the number of nearest neighbors), demonstrating that this can lead to major corrections to the Debye form and to very large Boson peaks. This is in general agreement with the idea that the scenario of glass-formation can be encoded by the changing coordi-

nation numbers as a function of temperature (so-called upscaling [5, 6, 7, 8, 9, 10, 11]). In Section VI the elastic moduli and the Debye frequencies which define the 'Debye point' are discussed. In Section VII we offer a summary of the paper and some concluding remarks.

II. DEBYE'S MODEL AND THE BOSON PEAK

A. Debye's Model

For the sake of simplicity in comparing with experimental results, Einstein employed a minimal model in which all the oscillators have the same frequency ω_E [1]. Then $g(\omega) = \delta(\omega - \omega_E)$ and the specific heat is given by:

$$C_V = dNk_B\left(\frac{\theta_E}{2T}\right)^2 csch^2\frac{\theta_E}{2T}, \tag{3}$$

where $\theta_E \equiv \hbar\omega_E/k_B$ is the so-called Einstein temperature. This minimal model agreed qualitatively with experimental observations of the specific heat; nevertheless careful measurements show that the low temperature behavior of (3) for a three-dimensional solid, i.e. $C_V \sim 3Nk_B(\theta_E/T)^2 exp(-\theta_E/T)$ falls off faster than experimental values. To explain the observed data one needs to account for more adequate vibrational spectra of actual solids. Debye was the first to link the oscillator frequencies in (1) with the collective vibrations of the solid. He treated a solid as an elastic isotropic continuum and estimated the density of vibrational states for the case of a spherical body [12]. Later it was shown that the frequency distribution is independent of the shape if the size of a body is large enough and the surface contribution can be neglected [13]. The modern simple derivation of the Debye distribution can be found, e.g., in [14]. The main statement of the continuum approximation is the linear dispersion relation between the frequency and the absolute value of the wave vector k, $\omega = u_s k$ where u_s is the sound velocity. In an isotropic body there exist one longitudinal and $d-1$ transverse sound waves, therefore, for spatial dimension $d > 1$ one needs two dispersion relations. The Debye density of states is given by:

$$g(\omega) = \begin{cases} \frac{d}{\omega_D}(\frac{\omega}{\omega_D})^{d-1} & \text{, if } \omega \le \omega_D \\ 0 & \text{, if } \omega > \omega_D, \end{cases} \tag{4}$$

where ω_D is the Debye frequency which defines the cut-off frequency in the spectrum:

$$\frac{1}{(\omega_D)^d} = \frac{\Omega_d}{(2\pi)^d \rho d}\left(\frac{1}{(u_l)^d} + \frac{d-1}{(u_t)^d}\right). \tag{5}$$

Here $\Omega_d = (\pi^{d/2})/\Gamma(1 + d/2)$ is the coefficient in the volume definition of d-dimensional hypersphere of radius r, $V_d = \Omega_d r^d$, $\Gamma(x)$ is the gamma function, ρ is the particle number density, u_l and u_t are the speeds of propagation of longitudinal and transverse sound waves:

$$u_l = \sqrt{\frac{dK + 2(d-1)\mu}{dm\rho}}; \quad u_t = \sqrt{\frac{\mu}{m\rho}}, \tag{6}$$

where K and μ are the bulk and shear moduli respectively and m is the molecular mass.

Debye's model has the advantage of a simple analytical form depending on the elastic properties of a solid only. Due to the long-wavelength approximation it is insensitive to the microscopic structure. Nevertheless experimental measurements indicated from the start that Debye's model is far from being the end of the story.

B. The Boson Peak

The vibrational properties of solids can be investigated experimentally by studying the inelastic interactions of external radiation with the solid vibrations. For inelastic scattering of photons one observes the Raman effect, discovered by Raman in liquids [15] and by Landsberg and Mandelstam in crystals [16]. As a result of this effect the frequency of the incident photon is either red shifted (Stokes scattering, with high amplitude) or blue shifted (anti-Stokes scattering, with low amplitude).

In crystals, due to the periodic structure, selection rules give rise to a discrete set of lines. In amorphous materials these spectral lines broaden, giving rise to a continuous spectrum. The Raman line shape was related to the density of states of amorphous materials in [17] under some assumptions in the harmonic approximation. The result can be rewritten for Stokes scattering in the following form:

$$\frac{I_{exp}(\omega)}{\omega[n(\omega, T) + 1]} = C(\omega)\frac{g(\omega)}{\omega^2}, \tag{7}$$

where $I_{exp}(\omega)$ is the observed Raman intensity at the frequency shift equal to ω and

$$n(\omega) = \frac{1}{exp(-\frac{\hbar\omega}{k_B T}) - 1} \tag{8}$$

is the Bose distribution function. The function $C(\omega)$ is an empirical function called "the average light vibration coupling constant". Thus the right-hand side of Eq. (7) is independent of temperature, meaning that the temperature dependence of the Raman intensity should be compensated by the temperature dependence of the Bose distribution function. This conclusion was confirmed by experiments (see e.g. [18]). At low frequencies the Raman spectrum has a bump whose amplitude changes with temperature. Once scaled by the Bose function the data at different temperatures collapse to a temperature-independent peak, which is therefore usually referred to as the 'Boson peak'.

Analysis of Raman spectra for different amorphous materials indicates the existence of a Boson peak [19].

Therefore, it was suggested that Raman spectra indicate some universal features of amorphous systems, independent of the details of molecular interactions. Unfortunately, experimental results determine only the product of the density of states and the light-vibrational coupling constant, cf. Eq. (7). Under the assumption that the low-frequency density of state is defined by the Debye model, for three-dimensional systems we have $g(\omega)/\omega^2 = const$. In this case, and only in this case, Eq. (7) implies that the coefficient $C(\omega)$ [19] must exhibit the Boson peak. On the other hand if the Debye model does not apply to the particular material at hand, this conclusion cannot be reached.

Additional light was shed on this problem using inelastic scattering of cold neutrons [13]. Such experiments indicate that in amorphous solids at small frequencies the quantity $g(\omega)/\omega^2$ is *not* constant, showing an excess in the vibrational density of states [20, 21]. The vibrational density of states defines the temperature dependence of the specific heat (1) and indeed the latter quantity also displays an excess at low temperature amorphous solids compared to the prediction of Debye's model. This again provides evidence for additional contributions to the vibrational density of states [22].

At present it is clear (see, e.g. [23]) that the Raman coupling coefficient $C(\omega)$ is a rather complicated monotonic function of frequency. Therefore, the peak in (7) is defined by the non-monotonic behavior of the density of vibrational states at low frequencies (in the sense of Raman scattering). The term 'Boson peak' is transferred from the Raman intensity to the shape of the vibrational density of states at low frequencies. In other words, the Boson peak describes the *deviation* (excess) from the expected constancy of $g(\omega)/\omega^{d-1}$ in the d-dimensional Debye model.

Once we define the problem of the Boson peak as equivalent to finding the deviations from the Debye model, the Boson peak is no longer special to amorphous solids. Debye's model takes into account only homogeneous elastic effect; after all, it is well known that the vibrational spectra of crystals have maxima at the van Hove singularity points and these maxima are independent of the temperature. The spectral properties in these regions are defined only by the lattice structure and the dimensionality (see, e.g., the well-known exact solution Eq. (23) below).

Disorder brings about additional deviations from the Debye model and different kinds of disorder have different effects on the density of states. We will show below that in one-dimensional systems disorder of the interparticle interactions induces a frequency redistribution with smoothing of the van Hove singularity. The peak of the spectrum moves to low frequencies with a shift which depends on the distribution of interactions. The same results were obtained by direct solution of Eq. (19) below for three-dimensional cubic lattices with spring constants distributed in accordance with a Gaussian [24] or other distributions [25] (in contrast to one-dimensional chains, three-dimensional cubic lattices are stable even if some of the spring constants are zero or negative). These and other results using the coherent potential approximation [26] lead to a conclusion that the 'Boson peak' in disordered systems is associated with the lowest van Hove singularity in the spectrum of the reference crystal [27].

It is important to stress that all these results can be taken only as a general indication for the appearance of the 'Boson peak' in amorphous solids in two or three dimensions. In all these models only nearest neighbor harmonic interactions (spring constants) were considered. For cubic lattices in two and three dimensions such interaction cannot give rise to a shear modulus, and only the bulk modulus is non-zero. Next-nearest-neighbor interaction are necessary for having a non-zero shear modulus.

III. BEYOND THE DEBYE MODEL: A FAIR WARNING

A more general microscopic model of vibrations in a solid was proposed by Born and von Kármán [28]. In the frame of this model it is assumed that all the atoms in a crystal interact with spring-like forces and that they vibrate near fixed equilibrium positions. This harmonic approximation can be used both for crystals and amorphous solids; however, an analytical solution can be obtained only for very simple cases of regular crystal structures.

The total potential energy of a particle configuration $R = \{\vec{r}_1, \vec{r}_2, \ldots, \vec{r}_N\}$ is expressed in a pairwise approximation as a sum over pair potentials:

$$U_R = \frac{1}{2}\sum_{i\neq j}\phi(r_{ij}). \tag{9}$$

Relative particle positions are given by vectors $\vec{r}_{ij} = \vec{r}_j - \vec{r}_i$, the distance between the ith and jth particles is $r_{ij} = |\vec{r}_{ij}|$. Small displacements of all particles $\vec{r}_i \to \vec{r'}_i = \vec{r}_i + \delta\vec{r}_i$ lead to a new configuration $R' = \{\vec{r'}_1, \vec{r'}_2, \ldots, \vec{r'}_N\}$ with the total potential energy:

$$U_{R'} = \frac{1}{2}\sum_{i\neq j}\phi(|\ \vec{r}_{ij} + \delta\vec{r}_{ij}\ |), \tag{10}$$

where:

$$\delta\vec{r}_{ij} = \delta\vec{r}_j - \delta\vec{r}_i. \tag{11}$$

We use the Taylor expansion

$$\phi(|\vec{r}+\delta\vec{r}|) = \phi(r)+(\delta\vec{r}\cdot\nabla)\phi(r)+\frac{1}{2}(\delta\vec{r}\cdot\nabla)^2\phi(r)+\ldots \tag{12}$$

to obtain

$$U_{R'} = U_R + \frac{1}{2}\sum_{i\neq j}\frac{\phi'(r_{ij})}{r_{ij}}\vec{r}_{ij}\cdot\delta\vec{r}_{ij} + \frac{1}{4}\sum_{i\neq j}\delta\vec{r}_{ij}\cdot\hat{\mathcal{I}}_{ij}\cdot\delta\vec{r}_{ij}, \tag{13}$$

where

$$\hat{\mathcal{T}}_{ij} = \left(\phi''(r_{ij}) - \frac{\phi'(r_{ij})}{r_{ij}}\right)\vec{n}_{ij} \otimes \vec{n}_{ij} + \frac{\phi'(r_{ij})}{r_{ij}}\mathcal{I} \quad (14)$$

is a symmetric tensor $\hat{\mathcal{T}}_{ij} = \hat{\mathcal{T}}_{ji}$, $\vec{n}_{ij} = \vec{r}_{ij}/r_{ij}$, and $\mathcal{I}$ is the identity tensor.

Substitution of (11) to (13) yields the dependence the energy of a harmonic system on particle displacements:

$$U_{R'} = U_R - \sum_i \vec{\mathcal{F}}_i \cdot \delta\vec{r}_i + \frac{1}{2}\sum_{i,j} \delta\vec{r}_j \cdot \hat{\mathcal{D}}_{ij} \cdot \delta\vec{r}_i. \quad (15)$$

Here the force applied to the ith particle is defined by:

$$\vec{\mathcal{F}}_i = \sum_{j\neq i} \phi'(r_{ij})\vec{n}_{ij} \quad (16)$$

and the dynamical matrix is given by

$$\hat{\mathcal{D}}_{ij} = \begin{cases} \sum\limits_{k\neq i} \hat{\mathcal{T}}_{ik} & \text{, if } i = j \\ -\hat{\mathcal{T}}_{ij} & \text{, if } i \neq j \end{cases} \quad (17)$$

The equations of motion for a harmonic solid follow from (15):

$$m_i \frac{\mathrm{d}^2\delta r_i^\alpha}{\mathrm{d}t^2} = \mathcal{F}_i^\alpha - \sum_{j,\beta} \hat{\mathcal{D}}_{ij}^{\alpha\beta} \cdot \delta r_i^\beta, \quad (18)$$

where m_i is the mass of ith particle and $1 \leq \alpha, \beta \leq d$. In equilibrium $\mathcal{F}_i^\alpha = 0$ and these equations are simplified.

Substitution of a particle displacement of the form $\delta r_i^\alpha = u_i^\alpha exp(-i\omega t)$ reduces Eqs. (18) to the eigenvalue problem:

$$\omega^2 u_i^\alpha = \frac{1}{m_i}\sum_{j,\beta} \hat{\mathcal{D}}_{ij}^{\alpha\beta} \cdot u_j^\beta \quad (19)$$

This equation can be solved directly by diagonalizing $\hat{D}_{ij}^{\alpha\beta}$ for a system of N particles when N is not too large. Binning the resulting eigenvalues leads to a histogram that approximates the density of states. The simplest example is the d-dimensional cubic lattice with unstressed distance a between adjacent lattice points at zero pressure. In the approximation of nearest-neighbor interactions with spring constants $\phi''(a) = \gamma$, the matrix (14) is given by:

$$\hat{\mathcal{T}}_{l^\alpha m^\alpha}^{\alpha\alpha} = \begin{cases} \gamma & \text{, if } \mid l^\alpha - m^\alpha \mid = 1 \\ 0 & \text{, otherwise,} \end{cases} \quad (20)$$

where a particle position is defined by the d-dimensional vector $\vec{la}$ with components $\{l^\alpha a\}$ where l^α are integer numbers. For this case the density of states can be found analytically [13] in the form of an inverse Laplace transform,

$$g(\omega) = 2\omega \frac{1}{2\pi i}\int_{\sigma-i\infty}^{\sigma+i\infty} e^{\omega^2 s} F(s)\mathrm{d}s, \quad (21)$$

where the image function $F(s)$ is:

$$F(s) = \frac{1}{d} e^{-2d\tilde{\gamma}s} I_0^d(2\tilde{\gamma}s). \quad (22)$$

Here $\tilde{\gamma} = \gamma/m$ and I_0^d is the modified Bessel function of order zero [29]. The inverse Laplace transform in closed analytical form is defined for one and two dimensional systems, for example if $d = 1$ the density of states is given by:

$$g(\omega) = \begin{cases} \frac{2}{\pi}\frac{1}{\sqrt{\omega_{max}^2 - \omega^2}} & \text{, } 0 \leq \omega \leq \omega_{max} \\ 0 & \text{, } \omega > \omega_{max} \end{cases} \quad (23)$$

where $\omega_{max} = 2\sqrt{\tilde{\gamma}}$. This function diverges at $\omega = \omega_{max}$. This is a general property of the density of the vibrational states; for *periodic structures* there are integrable singularities (called van Hove singularities) of $g(\omega)$ ($d = 1, 2$) or its derivatives ($d = 3$). The positions and types of van Hove singularities depend on the spatial dimension and the topological properties of the crystal [13, 30]. The low frequency behavior of this density of states was computed in [13] with the final result

$$g(\omega) = \frac{2}{d^2\Gamma(d/2)}\frac{\omega^{d-1}}{(4\pi\tilde{\gamma})^{d/2}}\left(1 + \frac{1}{8\tilde{\gamma}}\omega^2 + \dots\right) \quad (24)$$

The comparison of (24) with the Debye result (4) shows that *the Debye model gives the first term in a more general expansion.* The softer the system is, the larger is the correction. Substitution of Eq. (24) to Eq. (1) allows to estimate corrections to Debye's specific heat (see, e.g., [31]). We note that even for a perfect cubic crystal the Debye model is not exact, and there can be significant deviations. Clearly when the crystal is not perfect or when disorder sets in the changes from the Debye limit can become much larger. Thus a blind comparison of any given density of states to the Debye limit may be unwarranted and can lead to spurious conclusions. We will come back to this issue when we discuss the Boson peak below.

IV. ONE-DIMENSIONAL DISORDERED CHAINS

Consider a one-dimensional harmonic chain with lattice spacing a and with random masses and spring constants as the simplest model of a disordered solid. In the nearest-neighbor approximation the interaction potential $\phi(r_{ij})$ is defined by:

$$\phi(r_{i,i+1}) = \frac{1}{2}\gamma_{i,i+1}(r_{i,i+1} - a)^2. \quad (25)$$

where $\gamma_{i,i+1}$ are random spring constants taken from a prescribed distribution $p(\gamma)$. In this case the definition (14) reads:

$$\hat{\mathcal{T}}_{ij}^{11} = \begin{cases} \gamma_{ij} & \text{, if } \mid i - j \mid = 1 \\ 0 & \text{, otherwise} \end{cases} \quad (26)$$

and Eqs. (19) are written as:

$$m_i\omega^2 u_i = -\gamma_{i-1.i}u_{i-1} + (\gamma_{i-1,i}+\gamma_{i,i+1})u_i - \gamma_{i,i+1}u_{i+1}. \quad (27)$$

Unfortunately, it is impossible to derive a dispersion relations from these equations and the analytical solution discussed above becomes meaningless. Nevertheless, the response of the system to an applied static force ΔP can be inferred from the equilibrium conditions which follow from (25):

$$\gamma_{i,i+1}(r_{i,i+1}-a) = \Delta P. \quad (28)$$

Summing Eqs. (28) yields the elongation of the chain:

$$\Delta L = \sum_i^{N-1} r_{i,i+1} - (N-1)a = \Delta P \sum_i^{N-1} \frac{1}{\gamma_{i,i+1}}. \quad (29)$$

It is suitable to introduce a quantity $\frac{1}{\gamma_{av}} = \langle\frac{1}{\gamma}\rangle$, then the bulk modulus defined by the condition (29) is given by:

$$K = \frac{\gamma_{av}}{\rho}. \quad (30)$$

We reiterate that γ_{av} is the harmonic average of γ. Substitution of (30) to (6) and to (5) yields the following Debye frequency:

$$\omega_D = \pi\sqrt{\frac{\gamma_{av}}{m}}\ . \quad (31)$$

If $\gamma_{av} > 0$ the Debye frequency has a finite value. Since the Debye model takes into account only the elastic properties of the material, it should be exact in the limit $\omega \to 0$ independently of the detailed structure of the material. In this limit every material is an elastic medium. Thus we expect $\lim_{\omega\to 0} g(\omega) = d/\omega_D$ in agreement with the general law (4). We refer to this limit as the "Debye point".

In the case $\gamma_{av} = 0$ the low frequency behavior of the density of states depends on the properties of the probability distribution function $p(\gamma)$ for spring constants [32]. If $p(\gamma)_{\gamma\to 0} \to const$ in contrast to the Debye model (4) the density of states exhibits the singular behavior $g(\omega)_{\omega\to 0} \sim \sqrt{-ln\omega}$. The density of states in the whole frequency region was obtained by Dyson in [33] analytically for a particular distribution of the ratio of the spring constants to the masses. Dyson introduced a set of new constants $\{\tilde{\gamma}_n\}$ defined by:

$$\tilde{\gamma}_{2n-1} = \frac{\gamma_{n,n+1}}{m_n}, \qquad \tilde{\gamma}_{2n} = \frac{\gamma_{n,n+1}}{m_{n+1}}, \quad (32)$$

and derived an analytic solution for the distribution

$$p_n(\tilde{\gamma}) = \frac{n^n}{\Gamma(n)}\tilde{\gamma}^{n-1}e^{-n\tilde{\gamma}}. \quad (33)$$

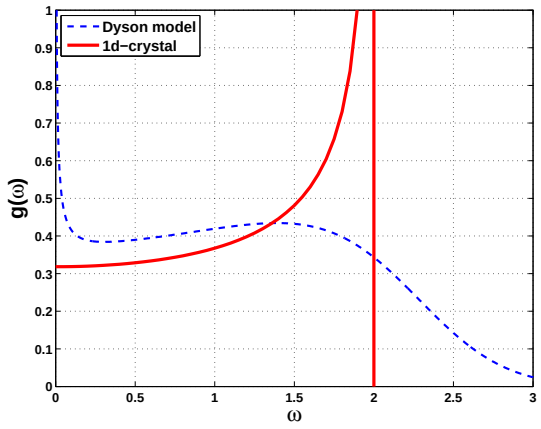

FIG. 1: Color Online: Density of vibrational states for a one-dimensional crystal (continuous line) and for exponentially distributed random interaction strength (dashed line).

The frequencies are measured in units of $\sqrt{\langle\gamma/m\rangle}$, and $\langle\tilde{\gamma}\rangle = 1$. For asymptotically large n, $p_n(\tilde{\gamma}) \to \delta(\tilde{\gamma}-1)$ which corresponds to the crystal state and the solution coincides with (23) [33].

The density of states for the a special case of the distribution (33) with $n = 1$ (exponential distribution) is shown in Fig. 1. It is known that disorder leads to smoothing out any van Hove singularity [26]. The Dyson solution shows that due to the smoothing out of the peak, states penetrate into the high-frequency region which is forbidden for the periodic structure. In the small-frequency regime this function diverges logarithmically in accordance with the general result of [32]. The frequencies are redistributed so that the zero-frequency singularity is followed by a dip. Such behavior is completely different from that of the Debye model.

Unfortunately, it is impossible to study the crossover from Debye to non-Debye behavior analytically. Nevertheless the density of states of one-dimensional disordered systems can be estimated with the help of the efficient numerical method proposed in [34] (extension for higher dimensions is discussed in [35, 36]). This method allows to calculate the number of frequencies less than ω using properties of a Sturm sequence [37]. In the following we present calculations pertaining to chains of 10^7 particles of identical mass $m = 1$; in order to compare different systems we enforced in all cases cases $\langle\gamma\rangle = 1$. The results are summarized as follows:

A. Uniform distribution.

The simplest distribution function (used also in [34] for chains of 10^3 particles) is the uniform distribution:

$$p_u(\gamma) = \begin{cases} \frac{1}{2\Delta} & \text{, if } 1-\Delta \le \gamma \le 1+\Delta \\ 0 & \text{, otherwise} \end{cases} \quad (34)$$

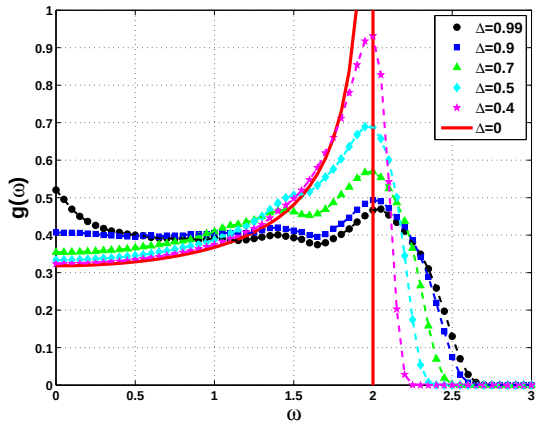

FIG. 2: Color online: Density of vibrational states for a one-dimensional chain with interactions distributed by the uniform distribution (34). Different symbols pertain to different values of the parameter Δ, see inset.

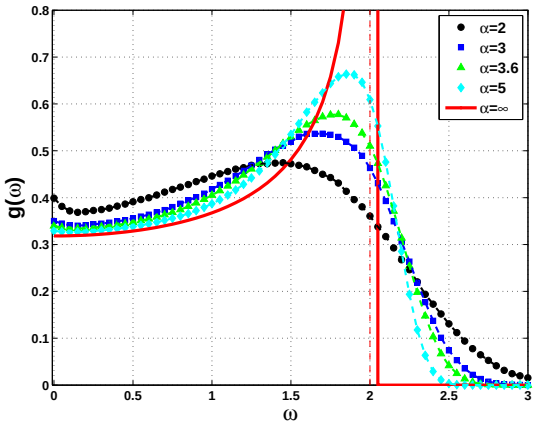

FIG. 3: Color online: Density of vibrational states for a one-dimensional chain with interactions distributed by the Weibull distribution (36). Different symbols pertain to different values of the parameter α, see inset.

For this distribution:

$$\gamma_{av} = \frac{2\Delta}{ln\frac{1+\Delta}{1-\Delta}}. \tag{35}$$

If $\Delta \to 0$ $p_u(\gamma) \to \delta(\gamma - 1)$ and the system is reduced to the homogeneous chain. If $\Delta \to 1$ the spring constant $\gamma_{av} \to 0$ and one can expect the divergence of $g(\omega)$ at vanishing frequencies.

The density of vibrational states for the uniform distribution is shown in Fig. 2. Upon increasing the parameter Δ the van Hove singularity at $\omega = 2$ in reduced units is smoothed out and then splits into two peaks moving in opposite directions. When Δ approaches unity the number of low frequency modes increases and a minimum at intermediate frequencies is formed.

B. Weibull distribution.

The Weibull distribution is defined by:

$$p_W(\gamma) = \frac{\alpha}{\lambda}\left(\frac{\gamma}{\lambda}\right)^{\alpha-1} e^{-(\frac{\gamma}{\lambda})^{\alpha}}. \tag{36}$$

The mean is given by:

$$\langle\gamma\rangle = \lambda\Gamma(1 + 1/\alpha) \tag{37}$$

and in order to obtain $\langle\gamma\rangle = 1$ the parameter λ was set to:

$$\lambda = \frac{1}{\Gamma(1 + 1/\alpha)}. \tag{38}$$

The average spring constant is given by:

$$\gamma_{av} = \frac{\alpha sin(\pi/\alpha)}{\pi}. \tag{39}$$

When the parameter $\alpha \to \infty$, $p_W(\gamma) \to \delta(\gamma - 1)$ and the chain becomes uniform. For $\alpha = 1$ the Weibull distribution degenerates to the exponential distribution and the results obtained in [33] are expected. The density of the vibrational states for the Weibull distribution with $\alpha > 1$ is shown in Fig. 3. In these cases one peak advances toward low frequencies, and in the vicinity of zero frequency another peak is developed.

C. Inverse distribution.

The exponential distribution of the logarithm of the spring constant was used in [25] for the investigation of the vibrations of a three dimensional disordered cubic lattice. This distribution is given by:

$$p_s(\gamma) = \begin{cases} \frac{1}{ln\lambda}\frac{1}{\gamma} & \text{, if } a \le \gamma \le \lambda a \\ 0 & \text{, otherwise} \end{cases} \tag{40}$$

The mean is $a(\lambda - 1)/ln\lambda$, therefore, the parameter a is defined by:

$$a = \frac{ln\lambda}{\lambda - 1}. \tag{41}$$

The average spring constant is given by:

$$\gamma_{av} = \lambda\left(\frac{ln\lambda}{\lambda - 1}\right)^2. \tag{42}$$

$\lambda = 1$ corresponds to the ordered chain. The densities of the vibrational states for the distribution (40) with different values of λ are shown in Fig. 4. For large λ a dip at low frequencies develops and is followed by a peak, both moving to smaller frequencies with increasing the parameter λ.

Finally, recall that the Debye behavior of a disordered chain is defined by its elastic properties (31), i.e., by γ_{av}.

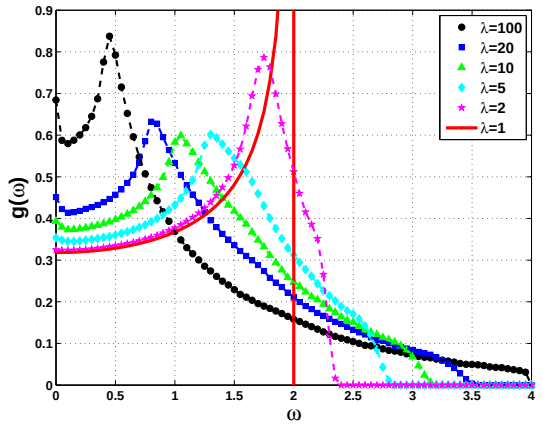

FIG. 4: Color online: Density of vibrational states for a one-dimensional chain with interactions distributed by the inverse distribution (40).Different symbols pertain to different values of the parameter λ, see inset.

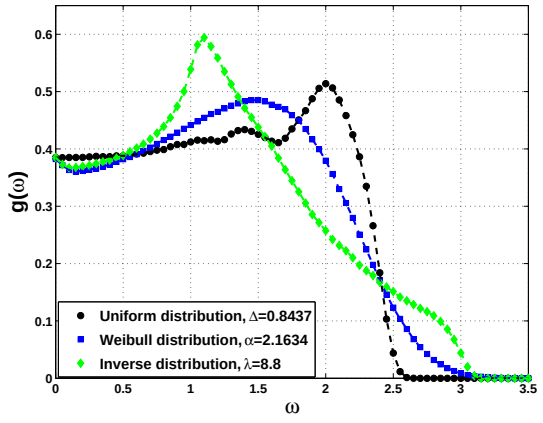

FIG. 5: Color online: Comparison of the vibrational density of states for a common value $\gamma_{av} = 0.6838$. The symbols are explained in the inset.

Therefore it is useful to compare vibrational properties of different chains with the same bulk modulus, cf. Fig. 5. Note that this figure is interesting from the point of view of comparing with Debye's model. The Debye point at $\omega = 0$ is the same for all three models since we chose γ_{av} to be the same; hence the Debye frequency (31) is identical for these three models. We could therefore expect identical Debye predictions for these three models. In contrast, the actual density of states presents widely different frequency dependence for the three models. This means that the re-distribution of frequencies depends on the nature of randomness and is not only a function of the elastic properties.

V. TWO-DIMENSIONAL SYSTEMS

In an amorphous solid the distance between two particles, their relative orientation, and the number of nearest and next-nearest neighbors of each particle all possess some randomness and thus all the terms in $\hat{\mathcal{T}}_{ij}$ are random and so are the elements of the dynamical matrix $\hat{\mathcal{D}}_{ij}$ in Eq. (19). In order to study the effect of different types of disorder on the spectrum of the dynamical matrix we examine several models of elastic networks.

A. Elastic triangular anti-ferromagnet

The anti-ferromagnetic Ising model on a rigid triangular lattice is geometrically frustrated since the energy of the three bonds on each triangular plaquette of the lattice may not be simultaneously minimized [38, 39]. This leads to a highly degenerate ground-state and thus to unconventional phases of matter [40, 41, 42, 43]. Allowing the lattice to deform may relieve this frustration and lift the ground-state degeneracy [44, 45]. Recent experimental [46] and theoretical [47] studies have shown that frustration is only partially relieved and that such systems exhibit glassy behavior, dramatically slow down, and fall into metastable disordered configurations. In order to allow the system to obtain a disordered deformation, we follow [48] and assume a pair potential for Eq. (9) of the form:

$$\phi_{ij}(r_{ij}) = -J\ \sigma_i\sigma_j\ [1-\epsilon\ (r_{ij}-a)] + \frac{1}{2}\gamma\ (r_{ij}-a)^2, \quad (43)$$

Here we assume the spin variables $\sigma_i = \pm 1$ are random. The magnetic interaction is taken to be anti-ferromagnetic $J < 0$, $\epsilon > 0$ controls the magneto-elastic coupling strength, and $\gamma > 0$ is the stiffness of the uniform springs connecting each nearest-neighbor pair. Note that some previous studies of the density of vibrational states of elastic networks (see for example [27]) focused on harmonic lattices with random spring constants (a multidimensional version of the one-dimensional analysis provided in Section IV). In the models we use here, the strength of the interaction is randomized by frustration and non-harmonic terms in the potential and therefore arises more naturally; we do not need any assumptions about the distributions that govern the interactions. In this sense the disorder in this model and its derivatives are similar in nature to the disorder in glass forming molecular systems. Another important difference with respect to conventional lattice models is the effect of off-lattice positional disorder on the terms that depend on the relative distance and orientation between two particles in the matrix $\hat{\mathcal{T}}_{ij}$, which in the present case reads

$$\hat{\mathcal{T}}_{ij} = \left(\gamma - \frac{J\ \sigma_i\sigma_j\ \epsilon + \gamma\ (r_{ij}-a)}{r_{ij}}\right)\vec{n}_{ij}\otimes\vec{n}_{ij}$$

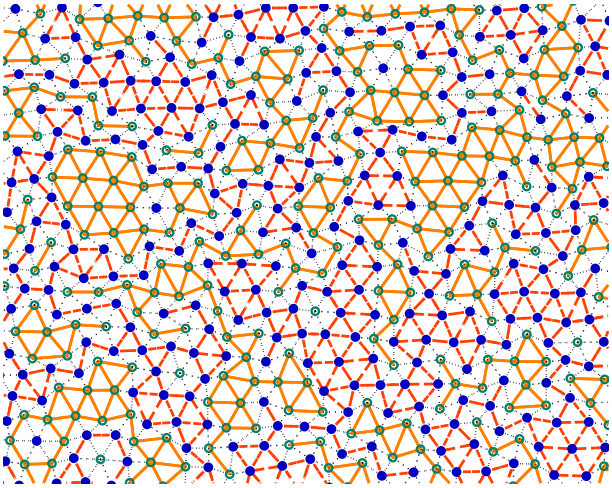

FIG. 6: Color online: Typical realization of the elastic triangular anti-ferromagnet (43). Solid points represent up spins and empty points represent down spins. dashed lines connect interacting up spins and solid lines connect interacting down spins. Dotted lines connect pairs of interacting up and down spins.

$$+\frac{J\ \sigma_i\sigma_j\ \epsilon+\gamma\ (r_{ij}-a)}{r_{ij}}\mathcal{I} \qquad (44)$$

We calculated the density of states for 20 realizations with 6400 particles each. Each realization of the system was initiated by positioning the particles on a triangular lattice with periodic boundary conditions. Each particle was assigned a random spin value and the energy of the entire network was minimized, using the conjugate-gradient method [49]. The minimization was achieved by changing the coordinates of the particles, keeping the interaction between the original nearest-neighbors only, and keeping the spin values fixed. A typical resulting configuration is shown in Fig. 6. The density of states was then calculated using the eigenvalue Eq. (19). The square-roots of the eigenvalues were collected in bins and the histogram recorded. To compute $g(\omega)/\omega$) the most precise method turned out to be calculating $g(\omega)/\omega \equiv 2G(\omega^2)$ where $G(\omega^2)$ is the histogram of the eigenvalues themselves. In order to compute $g(\omega)/\omega$ at $\omega = 0$ we employed Eq. (5) and the elastic moduli computed below. The same method was used for all the models listed below. Throughout, we set $\gamma = 1$, $m = 1$, $J = 1$, $a = 1$ and measure the density of states for various values of ϵ and of the other parameters defined for the subsequent models.

Figure 7 shows the effect of disorder on the distribution of angles θ between the inter-particle bonds and the $\hat{x}$ axis. This angle determine the value of the term $\vec{n}_{ij} \otimes \vec{n}_{ij}$. In a perfect triangular lattice these angles take six discrete values $\theta_i = \pi/3i$, $(0 \le i \le 5)$. In the disordered system these angles have a smooth distribution, and due to isotropy it is sufficient to consider the distribution of of the angles of one bond, say between $[-\pi/6, \pi/6]$.

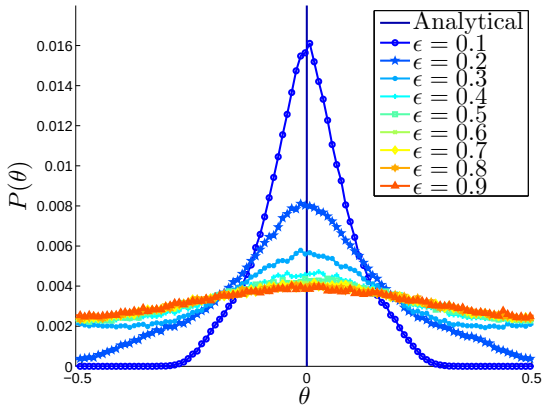

FIG. 7: Color online: Distribution of angles between nearest-neighbors in the elastic triangular anti-ferromagnet (43) for various values of ϵ, see inset.

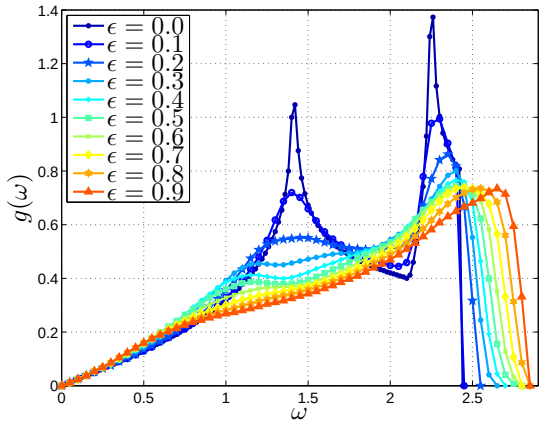

FIG. 8: Color online: Vibrational density of states in the elastic triangular anti-ferromagnet (43) for various values of ϵ, see inset.

Figure 8 shows the effect of disorder on the density of states. For the ordered triangular lattice the density of states exhibits van Hove singularities [50]. The most obvious effect of disorder is the smearing of the singularities and the flattening of the density of states. This results in filling the gaps between the singularities but also in some modes leaking to higher and lower frequencies. In particular, there is a change in the density of states at low-frequencies compared to the tail that characterizes the ordered lattice. It is important to note that when ϵ becomes too large, the network begins to fold upon itself. In a more realistic model, say with next-nearest-neighbor interactions, where the particles are not physically linked to each other this folding is relieved by changing the coordination number (i.e. number of neighbors). Below we will also study the effect of randomizing the coordination number.

To emphasize the deviation from Debye's model we examine in Fig. 9 the density of states divided by the prediction of Debye's model, which for $d = 2$ is linear

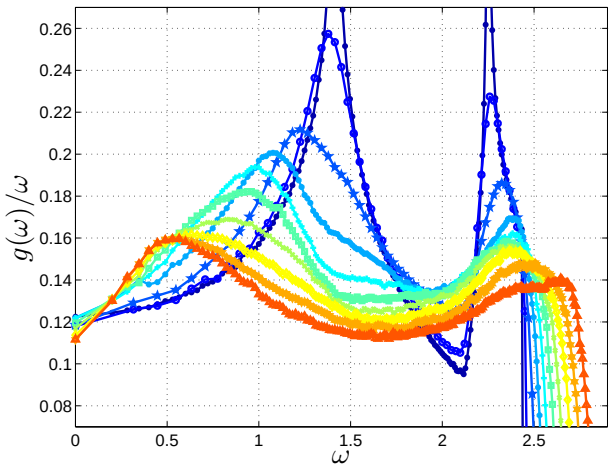

FIG. 9: Color online: Vibrational density of states normalized by Debye's prediction in the elastic triangular antiferromagnet (43). Symbols are the same as in Fig. 8

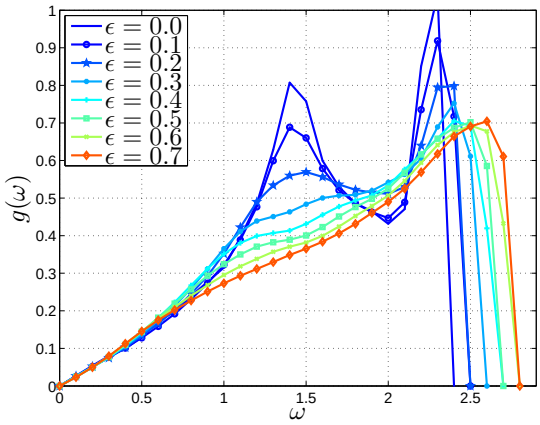

FIG. 10: Color online: Density of states for the model with non-linear elasticity (45) with $\kappa = 0.25$ and different values of ϵ, see inset.

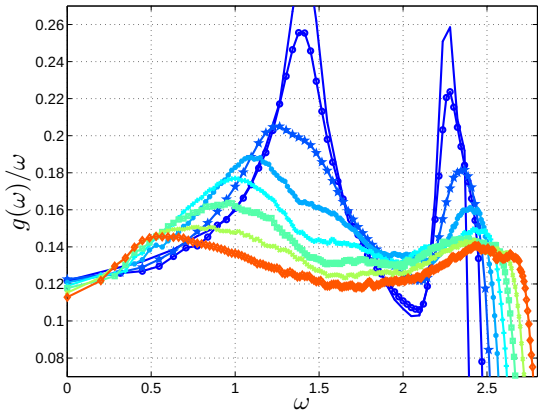

FIG. 11: Color online: Density of states for the model with non-linear elasticity (45) (Fig. 10) normalized by Debye's model. Symbols are the same as in Fig. 10

in frequency. A peak at low frequencies is observed and its position shifts to lower frequencies as the disorder increases. However, its height decreases upon increasing disorder. Thus *in this model there is a negative correlation between the magnitude of disorder and the amount of the deviation from the Debye model* (see also Figs. 2 and 3). Note that in this example it is hard to notice the deviation from the Debye model at low frequencies without dividing the density of states by ω.

Examining Figs. 8 and 9 we note that the density of states reaches zero at zero frequency in accordance with (4). Dividing by ω we observe a finite limit in Fig. 9. This behavior follows from Eq. (4) which predicts such a finite limit at $d = 2$.

B. Non-Linear Springs

Here we investigate the effect of random contributions to the harmonic part of the potential. This will bring us closer to generic systems. There is more than one way of doing so, and we therefore consider two different models for the inter-particle potential. The first has the form

$$\begin{aligned}\phi_{ij}(r_{ij}) &= -J\ \sigma_i\sigma_j\ [1-\epsilon\ (r_{ij}-a)] \\ &+ \frac{1}{2}\gamma\ (r_{ij}-a)^2+\frac{1}{3}\kappa\ (r_{ij}-a)^3 \end{aligned} \quad (45)$$

The harmonic term now reads:

$$\phi''(r_{ij}) = \gamma + 2\kappa(r_{ij}-a)\ . \quad (46)$$

Due to the fluctuation in the inter-particle distances around a, this term fluctuates around an average value γ.

We repeated the procedure described above for calculating the density of states for $\kappa = 0.25, 0.5$ and 1, and for various values of ϵ. We observed the same qualitative behavior for all κ values and present in Figs. 10 and 11 the raw density of states and the result after normalizing by Debye's prediction for $\kappa = 0.25$. As with the first model, we see excess modes at low frequencies

C. Magneto-elastic coupling

The second way to modify the elastic triangular antiferromagnet (43) is by adding a non-linear separation dependence to the magneto-elastic coupling term:

$$\begin{aligned}\phi_{ij}(r_{ij}) &= -J\ \sigma_i\sigma_j\ [1-\epsilon\ (r_{ij}-a)+\frac{1}{2}\nu(r_{ij}-a)^2] \\ &+ \frac{1}{2}\gamma\ (r_{ij}-a)^2. \end{aligned} \quad (47)$$

The harmonic term in this case reads:

$$\phi''_{ij}(r_{ij}) = \gamma - J\sigma_i\sigma_j\nu\ . \quad (48)$$

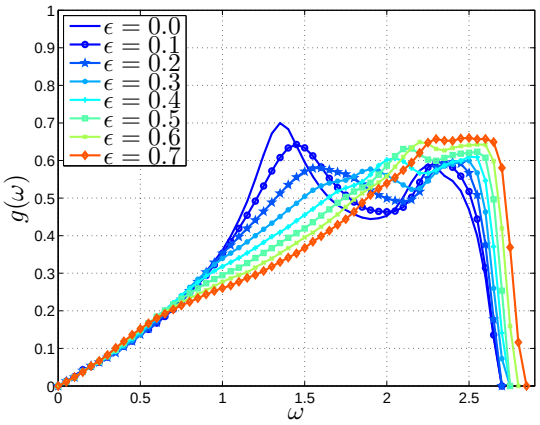

FIG. 12: Color online: Effect of the non-linear magneto-elastic coupling (47) on the density of states for $\nu = 0.3$ and different ϵ values, see inset.

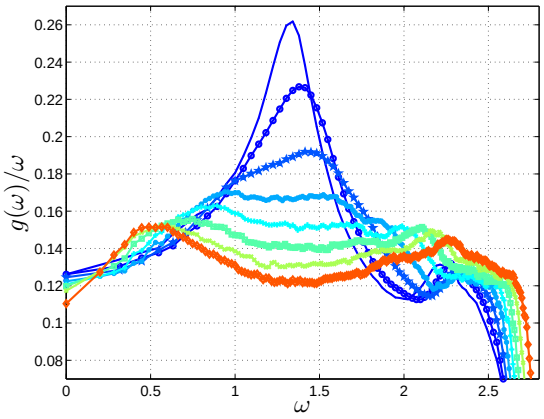

FIG. 13: Color online: The density of states with non-linear magneto-elastic coupling (Fig. 12) divided by the Debye behavior. The symbols are the same as in Fig. 12.

The density of states for this case is shown in Figs. 12 and 13 for a representative value of $\nu = 0.3$. Qualitatively similar results were obtained for $\nu = 0.45$. We recognize in these figures a smoothing of the Van-Hove singularities with redistribution toward both lower and higher frequencies. As before, we see a peak at low frequencies which moves toward lower frequencies when the disorder parameter ϵ is increased. We will next examine the effect of topological disorder and see that this type of disorder has a much more pronounced effect on the density of the low-frequency states.

D. Randomly diluted elastic triangular anti-ferromagnet

It has recently been argued that the glass transition involves a change in the number of neighbors that each particle has [5, 6, 7, 8, 9, 10, 11]. Moreover, recent work on jammed sphere packings has indicated the relevance of

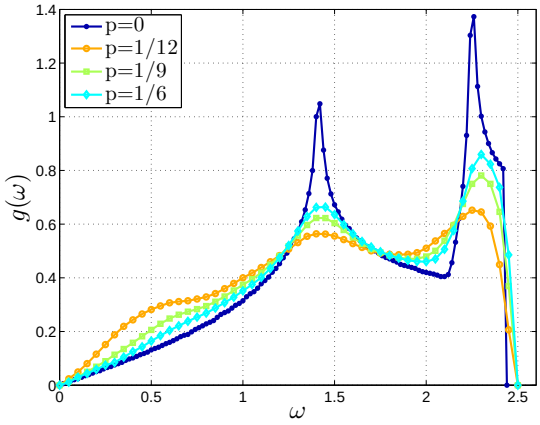

FIG. 14: Color online: Density of states of the diluted elastic triangular anti-ferromagnet (49) with $\epsilon = 0.1$ and various p values, as indicated in the inset.

the coordination number near isostaticity for determining low-frequency vibrational modes [51, 52, 53]. In order to account for these effects we use the elastic triangular anti-ferromagnet (43) but include the possibility of a missing link between two neighbors:

$$\phi_{ij}(r_{ij}) = g_{ij}\{-J\sigma_i\sigma_j[1-\epsilon\,(r_{ij}-a)]+\frac{1}{2}\gamma\,(r_{ij}-a)^2\} \quad (49)$$

Where g_{ij} is 0 with probability p and 1 with probability $1-p$. We use p close to 0 to avoid rigidity percolation [54, 55] and keep at least 3 bonds per particle in order to avoid floppy modes (modes of zero frequencies). We thus create a sparse network with a local coordination number varying between 6 and 3. This model is a modification of the model described in [56] which studied the effect of disconnecting links of a harmonic triangular lattice. In contrast to that model, our model introduces disorder in the equilibrium positions of the particles as well as in their coordination number. We solved this model as before, by first finding the lattice deformation that locally minimizes the mechanical energy. In this model the effect of disorder on the low-frequency domain of the density of states is much larger than before, as seen in Figs. 14 and 15.

The slope of the density of states at low frequencies, although linear, as expected by Debye's theory, is very different from the slope of the density of states for the perfect lattice (see also Fig. 4). However this modified Debye point is consistent with the system's elastic moduli, as will be descried in the following section.

VI. ELASTIC MODULI

To better understand the differences in types of randomness and their effect on the frequency redistribution we consider here the elastic moduli of the two-dimensional models treated above. Contrary to the density of states, the elastic moduli are global measures of

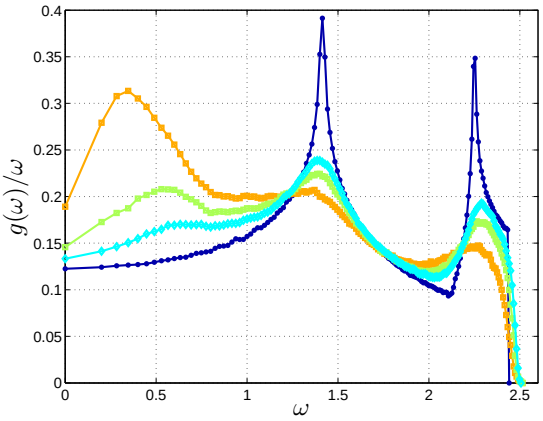

FIG. 15: Color online: Density of states of the diluted elastic triangular anti-ferromagnet (49) (Fig. 14) normalized by the Debye prediction. Symbols are the same as in Fig. 14.

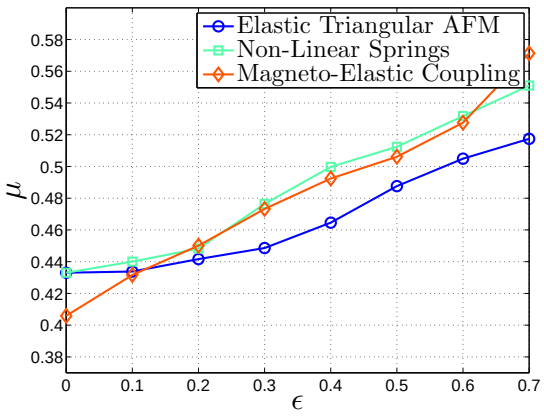

FIG. 16: Color online: Shear moduli of the three models Eqs. (43) (circles) , (45) (squares) and (47) (diamonds) for different values of the disorder control parameter ϵ.

the response of the system to external mechanical perturbations. Nevertheless there exists an interesting relation between these global properties and the frequency redistribution.

Measurements of the shear modulus were done by applying affine shear transformations, minimizing the energy after each step using the Lees-Edwards periodic boundary conditions, in order to measure the stress. After each minimization the stress for each particle was measured directly from its microscopic definition and the mean stress was computed as a sum over all particles. Next, the mean stress as a function of the strain was calculated, and the shear modulus was extracted from the numerical derivative. The bulk modulus was measured by decreasing the volume and measuring the diagonal part of the stress tensor (the pressure). The elastic moduli were used to calculate the Debye point at $\omega = 0$.

We first measured the elastic moduli for the first three models Eqs. (43), (45) and (47) for different values of ϵ (see Figs. 16 and 17). The results are somewhat unexpected. In all three models the shear modulus increases when disorder is increased, while the bulk modulus decreases. Thus in these three models we cannot say that the system softens or hardens, since one elastic modulus decreases while the other increases.

For the diluted network (49), both elastic moduli decrease with increasing p, see Figs. 18 and 19. This is very physical; cutting bonds must result in true softening of the system. Note that for a fixed value of p the qualitative behavior with ϵ is similar to the previous three models.

We see that this last model differs from the previous three in having clear softening when the parameter p increases. One way to take into account both moduli in discussing the softening of the system is by focusing on the Debye point

$$\lim_{\omega\to 0} \frac{g(\omega)}{\omega^{d-1}} = \frac{d}{(\omega_D)^d} \ . \qquad (50)$$

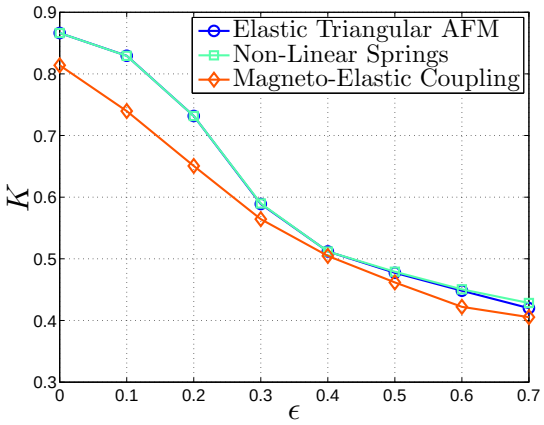

FIG. 17: Color online: Bulk modulus of the three models Eqs. (43) (circles) , (45) (squares) and (47) (diamonds) for different values of the disorder control parameter ϵ.

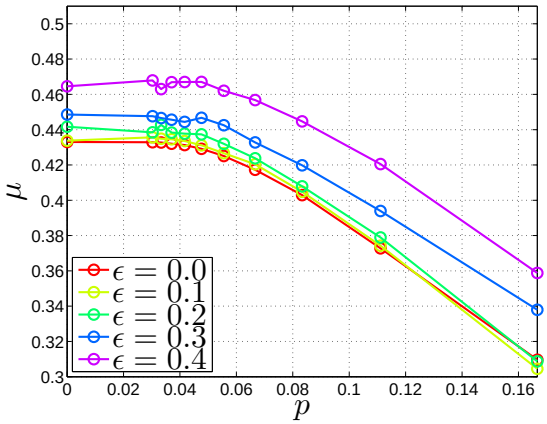

FIG. 18: Shear modulus of the diluted model Eq. (49) as a function of p and ϵ. The shear modulus increases when ϵ increase but it decreases when p increases.

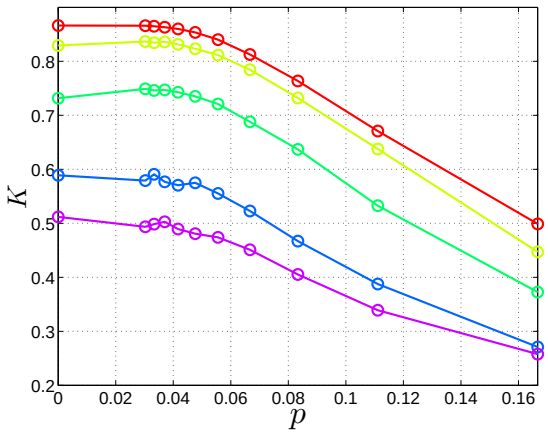

FIG. 19: Color online: Bulk modulus of the diluted model Eq. (49) as a function of p and ϵ, symbols as in Fig. 18. The bulk modulus decreases when ϵ increases but it decreases like the shear modulus when p increases.

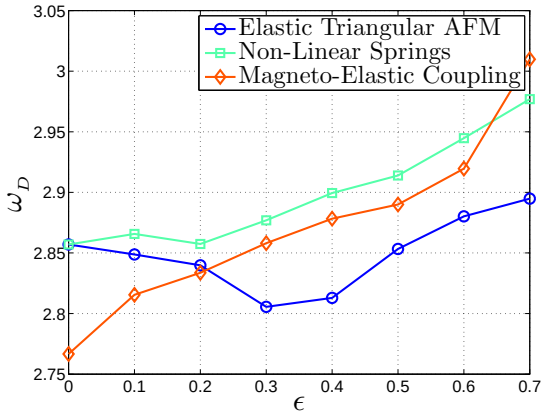

FIG. 20: The Debye frequency of the three models Eqs. (43) (circles) , (45) (squares) and (47) (diamonds) for different values of the disorder control parameter ϵ.

We computed the Debye frequency for the four models at hand, and the results are presented for the first three models in Fig. 20 and for the fourth model in Fig. 21.

We see from Fig. 20 that the Debye frequency is practically constant for the first model, and slightly increases with ϵ for the second and third models. For the fourth model (Fig. 21) the Debye frequency softens dramatically when the parameter p is changed. The disorder governed by the parameter ϵ almost does not change the Debye frequency also in this model.

VII. DISCUSSION AND CONCLUSIONS

The main conclusion from the one-dimensional and two-dimensional examples treated above are as follows:

1. Both ordered and amorphous solids exhibit peaks in their density of states. In ordered solids these peaks are understood as van Hove singularities. In amorphous solids these singularities are smoothed out, providing higher amplitudes to both lower and higher frequencies.

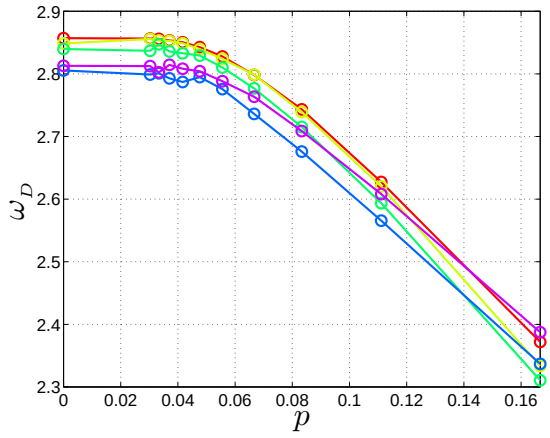

FIG. 21: Color online: The Debye frequency of the diluted model Eq. (49) as a function of p and ϵ, symbols as in Fig. 18.

2. For both the crystalline and the amorphous examples the comparison with the Debye model shows complete agreement only at $\omega \to 0$, independently of the dimensionality. Within the Debye model we expect $g(\omega)/\omega^{d-1}$ to be constant. This seems to be never the case.

3. Dividing the computed density of states by ω^{d-1} reveals the so-called "Boson peak". Its position and amplitude depend on many details; in one-dimensional cases we showed how it depends on the statistical distribution of the spring constants. In two-dimensions we showed how it depends mainly on the spatial disorder and on the coordination number, with the latter being dominant. In this sense there is nothing universal about the Boson peak. We cannot even tell a-priori whether increasing disorder might increase or decrease the amplitude of the Boson peak, cf. Fig. 22

4. We cannot discern any clear correlation between the Boson peak and the elastic moduli. In one dimension we showed (Fig. 5) that three models with identical bulk modulus exhibit completely different redistributions of frequencies. In two-dimensions we showed for the first three models that the bulk modulus decreased with disorder whereas the shear modulus increased, contrary to expectations. The change in the Debye frequency is small; nevertheless we have completely different frequency redistributions. In the fourth two-dimensional model we considered, both elastic moduli decrease simultaneously and we indeed saw a pronounced redistribution to lower frequencies when the average coordination number changed. Again we see no sys-

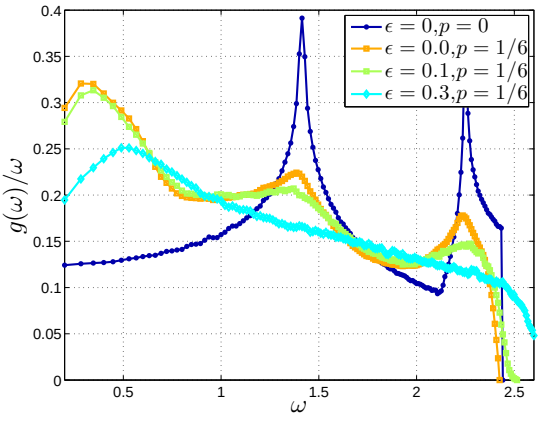

FIG. 22: Color online: $g(\omega)/\omega$) for the diluted model with different values of ϵ. Note that the Boson peak amplitude is reduced when ϵ which randomizes the particle positions is increased.

tematic correlation with the behavior of the elastic moduli.

Of course, all these conclusions concern the simple models discussed above. Nevertheless the phenomena discussed are not special to these models or even to amorphous solids in general. An experimental connection between shear modulus and the low-frequency behavior of the vibrational spectrum was given in [57] by analyzing the low-temperature specific heat. In contrast to the common view that excess in low-temperature specific heat (and, hence, in low-frequency modes) is special to disordered systems only, it was demonstrated that crystals and amorphous solids with almost the same shear modulus have quite different positions of the Boson peak. This is in accord with our conclusions that with the same Debye point we can have different redistributions of frequencies.

In summary, it is quite possible that in a given family of amorphous materials, where the randomness is quite similar, there can be a correspondence between the redistribution of frequencies and the shear modulus. However this is not a general correlation, as we saw with the present examples. We saw that the actual density of states is a complicated function of many competing influences. It is unlikely that one given parameter of whatever nature (like the shear modulus) can capture this full complexity. The understanding of the density of states and its changes under modified interactions remains a theoretical calculation of significant difficulty.

[1] A. Einstein, Ann. Phys. (Leipzig) **22**, 180 (1907).
[2] The role of this extension in the development of the quantum theory is discussed, e.g., in M.J. Klein, Science **148**, 173 (1965).
[3] See for example: V.L. Gurevitch, D.A. Parashin, H.R. Schober, Phys. Rev. B **67**, 094203 (2003).
[4] See for example: H. Shintani and H. Tanaka, Nature Materials bf 7, 870 (2008).
[5] E. Aharonov, E. Bouchbinder, V. Ilyin, N. Makedonska, I. Procaccia, and N. Schupper, Europhys. Lett. **77**, 56002 (2007).
[6] H.G.E. Hentschel, V. Ilyin, N. Makedonska, I. Procaccia, and N. Schupper, Phys. Rev. E **75**, 050404(R) (2007).
[7] V. Ilyin, E. Lerner, T.S. Lo, and I. Procaccia, Phys. Rev. Lett. 99, 135702 (2007).
[8] E. Lerner and I. Procaccia, Phys. Rev. E **78**, 020501(R) (2008).
[9] E. Lerner, I. Procaccia, and I. Regev, Phys. Rev. E **79**, 031501 (2009).
[10] E. Lerner, I. Procaccia, and J. Zylberg, Phys. Rev. Lett. **102**, 125701 (2009).
[11] L. Boué, E. Lerner, I. Procaccia, and J. Zylberg, Phys. Rev. E, submitted. arXiv:0905.3962
[12] P. Debye, Ann. Phys. **39**, 789 (1912).
[13] A.A. Maradudin, E.W. Montroll, and G.H. Weis, Theory of Lattice Dynamics in the Harmonic Approximation, edited by F. Seitz and D. Turnbull (Academic, New York, 1963).
[14] L.D. Landau and E.M. Lifshitz, *Statistical Physics* 3rd ed. (Pergamon, Oxford, 1980).
[15] C.V. Raman, Ind. J. Phys. **2**, 387 (1928).
[16] G.S. Landsberg and L.I. Mandelstam, Z. Phys. **50**, 769 (1928).
[17] R. Shuker and R.W. Gammon, Phys. Rev. Lett. **25**, 222 (1970).
[18] M. Hass, Solid State Comm. **7**, 1069 (1969).
[19] V.K. Malinovsky and A.P. Sokolov, Solid State Comm. **57**, 757 (1986).
[20] U. Buchenau, N. Nücker, and A.J. Dianoux, Phys. Rev. Lett. **53**, 2316 (1984).
[21] M.G. Zemlyanov, V.K. Malinovskii, V.N. Novikov, P.P. Parshin, and A.P. Sokolov, Pis'ma Zh. Eksp. Teor. Fiz. **49**, 521 (1989).
[22] N. Ahmad, K.W. Hutt, and W.A. Phillips, J. Phys. C: Solid State Phys. **19**, 3765 (1986).
[23] G. D'Angelo, G. Carni, C. Crupi, M. Koza, G. Tripodo, and C. Vasi, Phys. Rev E **79**, 014206 (2009).
[24] W. Schirmacher, G. Diezeman, and C. Ganter, Phys. Rev. Lett. **81**, 136 (1998).
[25] J.W. Kantelhardt, S. Russa, and A. Bunde, Phys. Rev. B **63**, 064302 (2001).
[26] J.M. Ziman, Models of Disorder (Cambrige University Press, Cambrige, 1979).
[27] S.N. Taraskin, Y.L. Loh, G. Natarajan, and S.R. Elliot, Phys. Rev. Lett. **86**, 1255 (2001).
[28] M. Born and T. von Kármán, Phys. Z. **13**, 297 (1912).
[29] Handbook of Mathematical Functions, Edited by M. Abramowitz and I. Stegun (National bureau of standarts, 1964).
[30] L. van Hove, Phys. Rev. **89**, 1189 (1953).
[31] R.B. Leighton, Rev. Mod. Phys. **20**, 165 (1948).
[32] S. Alexander, J. Bernasconi, W. R. Schneider, and R. Orbach, Rev. Mod. Phys. **53**, 175 (1981).
[33] F.J. Dyson, Phys. Rev. **92**, 1331 (1953).

[34] P. Dean, Proc. Phys. Soc. **84**, 727 (1964).
[35] P. Dean and J.L. Martin, Proc. Royal Soc. of London, Series A, **259**, 409 (1960).
[36] P. Dean, Rev. Mod. Phys. **44**, 127 (1972).
[37] A. Quarteroni, R.Sacco, and F.Saleri, Numerical Mathematics (Springer, 2000).
[38] G.H. Wannier, Phys. Rev. **79**, 357 (1950); Phys. Rev. B **7**, 5017 (1973).
[39] R.M.F. Houtappel, Physica **16**, 391 (1950); Physica **16**, 425 (1950).
[40] R. Moessner, Can. J. Phys. **79**, 1283 (2001).
[41] A.R. Ramirez, Nature **421**, 483 (2003).
[42] G. Tarjus, S.A. Kivelson, Z. Nussinov, and P. Viot, J. Phys.: Condens. Matter **17** R1143 (2005).
[43] R. Moessner and A.R. Ramirez, Phys. Today **59**, 24 (2006).
[44] Z.Y. Chen and M. Kardar, J. Phys. C: Solid State Phys. **19**, 6825 (1986).
[45] L. Gu, B. Chakraborty, P.L. Garrido, M. Phani, and J.L. Lebowitz, Phys. Rev. B **53**, 11985 (1996).
[46] Y. Han, Y. Shokef, A.M. Alsayed, P. Yunker, T.C. Lubensky, and A.G. Yodh, Nature (London) **456**, 898 (2008).
[47] Y. Shokef and T.C. Lubensky, Phys. Rev. Lett. **102**, 048303 (2009)
[48] Y. Shokef, A. Souslov, and T.C. Lubensky, in preparation.
[49] Modified from the program macopt written by David J.C. MacKay and Steve Waterhouse, downloaded from http://www.inference.phy.cam.ac.uk/mackay/c/macopt.html.
[50] P. Dean, Proc. Cambridge Phil. Soc. **59**, 383 (1963).
[51] L.E. Silbert, A.J. Liu, and S.R. Nagel, Phys. Rev. Lett. **95**, 098301 (2005).
[52] M. Wyart, Ann. Phys. (Paris) **30**, 1 (2005).
[53] N. Xu, M. Wyart, A.J. Liu, and S.R. Nagel, Phys. Rev. Lett. **98**, 175502 (2007).
[54] S. Feng and P.N. Sen, Phys. Rev. Lett. **52**, 216 (1984).
[55] E.J. Garboczi and M.F. Thorpe, Phys. Rev. B **32**, 4513 (1985).
[56] S. Feng, M.F. Thorpe, and E. Garboczi, Phys. Rev. B **31**, 276 (1985).
[57] D.J. Safarik, R.B. Schwarz, and M.F. Hundley, Phys. Rev. Lett. **96**, 195902 (2006).